

# Traffic-load-induced dynamic stress accumulation in subgrade and subsoil using small scale model tests

Lian Sheng Tang<sup>\*1,2</sup>, Hao Kun Chen<sup>1</sup>, Yin Lei Sun<sup>1</sup>, Qing Hua Zhang<sup>1</sup> and Hua Rong Liao<sup>1</sup>

<sup>1</sup>Department of Earth Science and Geological Engineering, Sun Yat-sen University, No. 135 Xingang Road West, Guangzhou 510275, Guangdong Province, China

<sup>2</sup>Guangdong Provincial Key Laboratory of Geological Processes and Mineral Resources Survey, Guangzhou 510275, China

(Received December 8, 2016, Revised November 24, 2017, Accepted May 12, 2018)

**Abstract.** Under repeated loading, the residual stresses within the subgrade and subsoil can accelerate the deformation of the road structures. In this paper, a series of laboratory cyclic loading model tests and small-scale model tests were conducted to investigate the dynamic stress response within soils under different loading conditions. The experimental results showed that a dynamic stress accumulation effect occurred if the soil showed cumulative deformation: (1) the residual stress increased and accumulated with an increasing number of loading cycles, and (2) the residual stress was superimposed on the stress response of the subsequent loading cycles, inducing a greater peak stress response. There are two conditions that must be met for the dynamic stress accumulation effect to occur. A threshold state exists only if the external load exceeds the cyclic threshold stress. Then, the stress accumulation effect occurs. A higher loading frequency results in a higher rate of increase for the residual stress. In addition to the superposition of the increasing residual stress, soil densification might contribute to the increasing peak stress during cyclic loading. An increase in soil stiffness and a decrease in dissipative energy induce a greater stress transmission within the material.

**Keywords:** subgrade; subsoil; dynamic stress; accumulation; traffic load; time-dependent

## 1. Introduction

The subgrade and subsoil beneath road, railway and airport pavement are subjected to long-term repeated loads. The mechanical behavior of the soil under repeated loading differs significantly from the mechanical behavior of the soil under static loading (Sas *et al.* 2017). Failure may occur when the subgrade and subsoil are subjected to repeated loads that are considerably lower than the static strength of the subgrade and subsoil (Guo *et al.* 2013, Shahu *et al.* 2000). The negative influence of traffic loads on the subgrade structure is derived from the repetition of the loads (Hendry *et al.* 2013; Hu 2010). Under repeated loading, the cumulative deformation and residual stresses within the subsoil and subgrade may accelerate the deformation of the entire pavement and foundation structure, inducing pavement failure and even transportation accidents (Cui *et al.* 2014, Puppala *et al.* 2009, Werkmeister *et al.* 2005).

In road and foundation engineering, the stress increments in a soil mass due to various types of external loads on the ground are referred to as additional stress. Specifically, the dynamic stress response in the foundation induced by a moving vehicle or vibrating equipment is referred to as dynamic additional stress (abbreviated as dynamic stress) (Tang *et al.* 2015). Differing from the

external loads applied in element tests (such as a one-dimensional consolidation test or triaxial compression test), the dynamic additional stress is a stress response inside the material. In this paper, the vertical stress components were mainly concerned because these components are considered to be the major source of foundation settlement. Some terms relevant to the dynamic additional stress are residual stress (the additional stress remaining in the soil after unloading) and peak stress (the maximum additional stress response in a single loading cycle).

Tang *et al.* (2009, 2015) noted that the vertical stress responses in subgrade soils increased during vehicular loading. They conducted a field test and found that the vertical stresses in the subgrade increased rapidly in the initial stage of the cyclic loading, after which these vertical stresses tended to stabilize. This phenomenon is important because an increase in the stress response in the foundation accelerates the deformation of the subgrade structure.

As summarized in Table 1, in recent years, in situ monitoring tests (Tang *et al.* 2008), field tests (Wiermann *et al.* 1999, Shoop *et al.* 2009, Tang *et al.* 2015) and model tests (Eguchi and Muro 2007, Zhang *et al.* 2009, Garg *et al.* 2010, Thakur *et al.* 2012, Lu *et al.* 2012, Li and Liu 2014, Sun *et al.* 2015) have also suggested that an increase in peak stress in the base, subgrade and subsoil occurs when the pavement or ground is subjected to repeated loads. For example, Thakur *et al.* (2012) conducted a cyclic plate loading test on a base layer and demonstrated that the dynamic peak stresses in the clayey sand subgrade increased sharply in the first few cycles. The dynamic stresses then stabilized or continued to increase until soil

---

\*Corresponding author, Professor  
E-mail: [eestls@mail.sysu.edu.cn](mailto:eestls@mail.sysu.edu.cn)

Table 1 Literature review of the dynamic stress accumulation phenomenon in the foundation when the ground was subjected to repeat loads

Reference	Soil type	Test condition	Peak stress increased during repeated loading	Residual stress increased during repeated loading
Tang <i>et al.</i> (2015)	Clayey soil	Field test for the vertical stress response due to cyclic vehicular loads	Yes	No data
Tang <i>et al.</i> (2008)	Soft clay	In situ monitoring test for stress response due to subway vibration loads	Yes	Yes
Wiermann <i>et al.</i> (1999)	Norfolk sandy loam	Field test for the stress state influenced by cyclic wheel loads	Yes	No data
Shoop <i>et al.</i> (2009)	Silty sand, silt and clay	Field test for the 3D stress response due to repeated wheel loads	No data	Yes
Eguchi and Muro (2007)	Decomposed granite soil	Model test for the stress state influenced by a tracked vehicle carrying an oscillator	Yes	No data
Garg <i>et al.</i> (2010)	County sand and stone clay	Field test for the vertical stress response due to cyclic wheel loads	Yes	No data
Lu <i>et al.</i> (2012)	Cement stabilized gravel, completely decomposed granite	Model test for the vertical stress response due to cyclic semi-sinusoidal loads	Yes	No
Thakur <i>et al.</i> (2012)	Recycled asphalt pavement material and sand clay	Model test for the vertical stress response due to cyclic trapezoidal wave loads	Yes	No data
Li and Liu (2014)	Soft clay	Model test for the stress response in soil when applying the dynamic compaction method to strengthen the soil	Yes	Yes
Zhang <i>et al.</i> (2009)	Soft clay	Small scale model test for the vertical stress response in subsoil	Yes	Yes
Sun <i>et al.</i> (2015)	Sand and clay mixture	Model test for the response of vertical and horizontal stresses in the base course and subgrade due to cyclic loads	Yes	No data

failure occurred. Shoop *et al.* (2009) conducted a repeated loading test on silty sand, silt and clay. The results showed that the residual stresses occurred after unloading and that these stresses were superimposed on the subsequent loadings.

The aforementioned studies found that the residual stresses and peak stresses in the soil increased during cyclic loading. Abdelkrim *et al.* (2003) and Tang *et al.* (2015) suggested that the peak stress response is the superposition of a recoverable component due to the applied load and a residual stress. They noted that the accumulation of residual stresses, which were superimposed on the subsequent loading cycles, directly contributed to the increase in the peak stress response during repeated loading.

The cumulative deformation behavior of subgrade and subsoil under cyclic loading has been extensively investigated (Chai and Miura 2002, Suiker *et al.* 2005, Werkmeister *et al.* 2005, Liu and Xiao 2010, Mittal and Meyase 2012, Xiao *et al.* 2014, Ling *et al.* 2017, Sas *et al.* 2017), however, few studies have considered the accumulation effect of the residual stresses induced by traffic loading. Although some previous studies have found the phenomena of dynamic stress accumulation within soils either in the field tests or model tests, there are few further comprehensive studies on the mechanism and characteristics of dynamic stress accumulation under traffic

load. In this paper, certain laboratory model tests were conducted to investigate the influence of the loading amplitude, soil density and loading frequency together with certain small-scale model tests carried out to simulate the vehicular loading conditions in the aim to investigate the influence of the vehicular load, vehicle speed, loading frequency and soil properties. The accumulation effect of the stress response was emphasized within this essay. The main objective of this paper is to reveal the mechanism and characteristics of the accumulative effect of dynamic stress, compensating the deficiencies of dynamic stress accumulation researches and providing references for the upcoming researches.

## 2. Introduction to laboratory model tests and small-scale model tests

### 2.1 Experimental materials

Soft clay, granite residual soil and medium sand were used for the experimental investigations. The soils were sampled from a highway construction site in Guangzhou, China. The physical properties of the soils that were studied are shown in Table 2, and Fig. 1 describes the grain size distributions of the soils. In the natural state, the soft clay is nearly saturated and shows a soft plasticity. The sand soil included more than 50% grains with a diameter larger than 0.25 mm. The soft clay and granite residual soil used in the tests were disturbed soils.

### 2.2 Laboratory cyclic loading model test

The laboratory cyclic loading model tests were conducted to investigate the influence of loading amplitude, soil density and loading frequency on the accumulation effect of the deformation behavior and stress response. The development of the stress response was of particular interest.

The custom-designed piece of equipment (Fig. 2) used for the experiments included a soil compression apparatus, cyclic loading apparatus, and measurement and control system.

#### 2.2.1 Soil compression apparatus

The soil compression apparatus consisted of a cylindrical mould (15.2 cm in diameter), proving ring, lifting jack and rigid frame. Soils were filled into the cylindrical mould and subjected to vertical compressive loads generated by the lifting jack. Soil specimens with different dry densities could be obtained by adjusting the compressive load.

#### 2.2.2 Cyclic loading apparatus

The core components of the cyclic loading apparatus were a lever pressure instrument and small electromagnetic vibration exciter. The lever pressure instrument could magnify the applied force by a factor of 10. The loading area of the soil was a circle with an area of  $1.9635 \times 10^{-3} \text{ m}^2$  (0.05m in diameter). The lever pressure instrument was described in detail in the China Standard for Soil Test Method (GB/T 50123-1999) and the China Verification

Table 2 Physical properties of the soils

Soil type	Specific density (kN/m <sup>3</sup> )	Natural water content (%)	Liquid limit (%)	Plastic limit (%)	Maximum dry density (kN/m <sup>3</sup> )
Soft clay	26.9	58~60	61.5	32.0	-
Granite residual soil	27.2	26~28	40.0	23.5	28
Medium sand	26.7	-	-	-	18

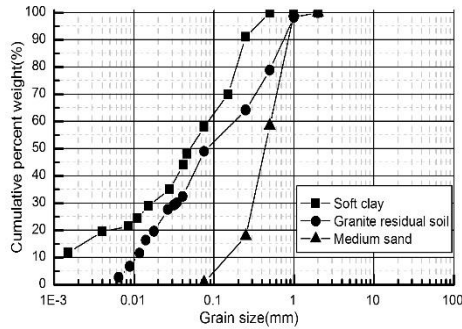
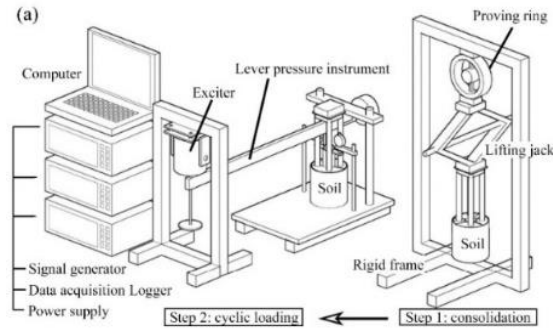
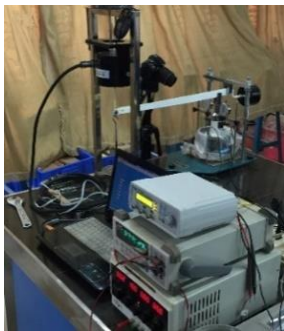


Fig. 1 Grain Size distribution curves of the soils used



(a) The schematic diagram of the test setup is drawn as above



(b) The photograph of the test equipment is taken as so  
 Fig. 2 The schematic diagram and photograph of the laboratory cyclic loading model test are illustrated hereby

Regulation of Lever Pressure Instrument (JJG107-2012). The electromagnetic vibration exciter could output a sinusoidal wave, a square wave, a triangular wave and other specified waves. The maximum excitation force and excitation frequency were 50 N and 0.01-10 kHz, respectively. The output excitation force of the vibration exciter was controlled by the electric current signals. After the vibration exciter was connected to the lever pressure instrument, the soil specimen could be subjected to a maximum cyclic load of 500 N (or 254.6 kPa).

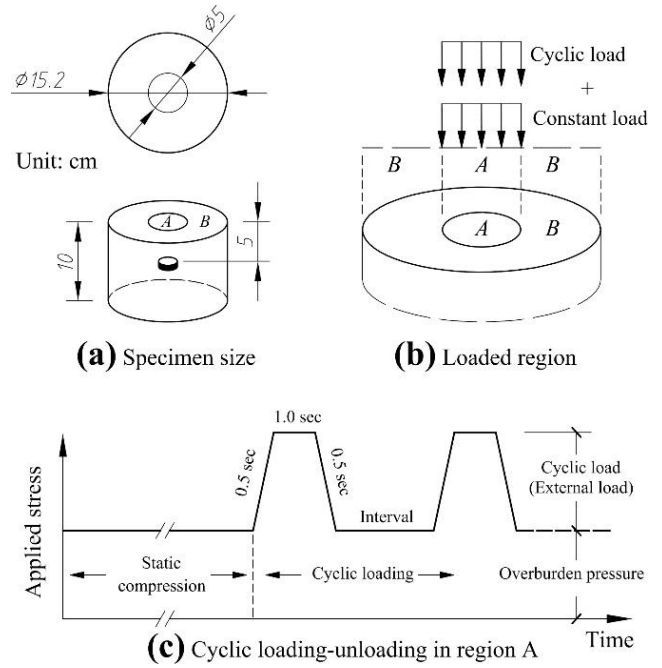


Fig. 3 Cyclic loads applied to the soil specimen in the laboratory model tests

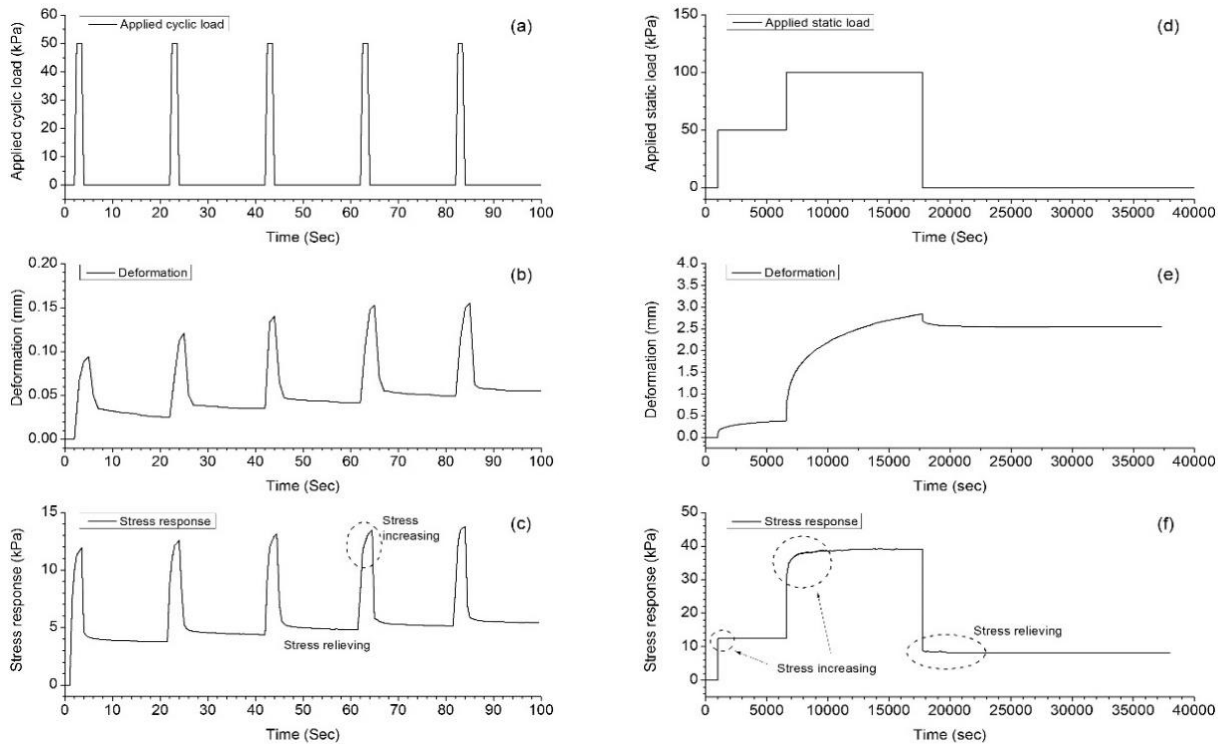
2.2.3 Measurement and control system

The control system consisted of a computer, a signal generator and the control software. The control system generated electric signals that controlled the magnitude and frequency of the output loads. The measurement system was used to monitor the dynamic response of the soil, including an earth pressure cell, two displacement gauges, a data logger and a computer. The earth pressure cell (made of stainless steel) was an electrical resistance strain type. The earth pressure cell had a diameter of 30 mm and a thickness of 8 mm. The accuracies of earth pressure cells and displacement gauges were 0.01 kPa and 0.01 mm, respectively. The capacity of earth pressure cell and displacement gauge were 100 kPa and 10 mm, respectively. The data logger was set to collect data at a frequency of 10 Hz. All of the sensors were calibrated before use.

2.2.4 Sample preparation and test procedure

Soils were filled into the cylindrical mould in layers, and the earth pressure cell was embedded into the middle and center of the soil. The earth pressure cell was horizontally installed to obtain the vertical stress. After the soil was fully filled into the mould, a vertical force was applied to compact the soil using the soil compression apparatus until the rate of soil settlement was less than 0.01 mm per hour. The soil specimens were approximately 0.1m high after compression.

Subsequently, the soil specimen (with the cylindrical mould) was installed in the lever pressure instrument. To minimize the frictional effect from the side wall, loads were applied only to the central circle area ( $1.9635 \times 10^{-3} \text{ m}^2$ ) of the soil specimen, as shown in Figs. 3(a) and 3(b). After the soil specimen was installed, a constant load of 100 kPa was applied to the soil specimen. The vibration exciter was connected to the lever pressure instrument, and cyclic loads



(a)-(c) applied cyclic load, deformation and dynamic stress response in the first few loading cycles of test C04

(d)-(f) applied constant load, deformation and stress response in the static loading test

Fig. 4 Dynamic response of the soil under cyclic loading conditions and static loading conditions

were applied to the soil specimen. The loading waves were trapezoidal, as shown in Fig. 3. The constant load was applied to simulate the overburden pressure in the field, whereas the cyclic load was applied to simulate the forces generated by moving vehicles. The “external load” or “cyclic load” denotes the cyclic stress amplitude (which was the total load minus the constant load), as shown in Fig. 3(c). The stress response within the soil and the vertical deformation were monitored during the cyclic loading.

### 2.2.5 Test plan

The test conditions for the laboratory cyclic loading model test are shown in Table 3. The influences of the loading frequency (Group One), soil dry density (Group Two) and loading amplitude (Group Three) on the cyclic performance of the soil were investigated. The tests were conducted mainly on soft clay, but a series of comparison tests was also conducted on unsaturated residual soil and sandy soil. Cyclic loadings were terminated after 2000 cycles. Before the next test, soil specimens were prepared and the measurement devices were reinstalled. In test C05, the constant load during the cyclic loading procedure was 100 kPa, although a static compressive stress of 250 kPa had been applied to obtain a higher soil density.

In addition, a special comparative experiment was also conducted to observe the internal stress response and soil deformation under static loading conditions. The specimen used in this test was the specimen that had been used in test C06. The loading conditions and the results of this static loading test are shown in Figs. 4(d)-4(f).

Table 3 Test conditions for the laboratory cyclic loading model tests

Soil	Test group	Test	Static compressive stress(kPa)	w* (%)	$\rho_d^*$ (kg/m <sup>3</sup> )	Cyclic load (kPa)	Frequency (Hz)	Control variables
Soft clay	Group One (C01-04)	C01	100	55.2	$1.10 \times 10^3$	20	0.10	loading frequency
		C02	100	54.5	$1.11 \times 10^3$	20	0.02	
		C03	100	55.0	$1.09 \times 10^3$	50	0.10	
		C04	100	54.0	$1.12 \times 10^3$	50	0.05	
Soft clay	Group Two (C03, 05)	C03	100	55.0	$1.09 \times 10^3$	50	0.10	soil dry density
		C05	250	46.0	$1.20 \times 10^3$	50	0.10	
Soft clay	Group Three (C01, 03, 06)	C06	100	53.2	$1.12 \times 10^3$	5	0.10	loading amplitude
		C01	100	55.2	$1.10 \times 10^3$	20	0.10	
		C03	100	55.0	$1.09 \times 10^3$	50	0.10	
Unsaturated granite residual soil	Group Four (C07, 08)	C07	100	23.8	$1.44 \times 10^3$	20	0.10	Soil type
		C08	100	24.5	$1.45 \times 10^3$	100	0.10	
Unsaturated medium sand	Group Five (C09, 10)	C09	100	5.1	$1.48 \times 10^3$	20	0.10	Soil type
		C10	100	4.8	$1.49 \times 10^3$	215	0.10	

\*Water content and dry density of the soil specimen after static compression

## 2.3 Small-scale model test

### 2.3.1 Introduction of small-scale model

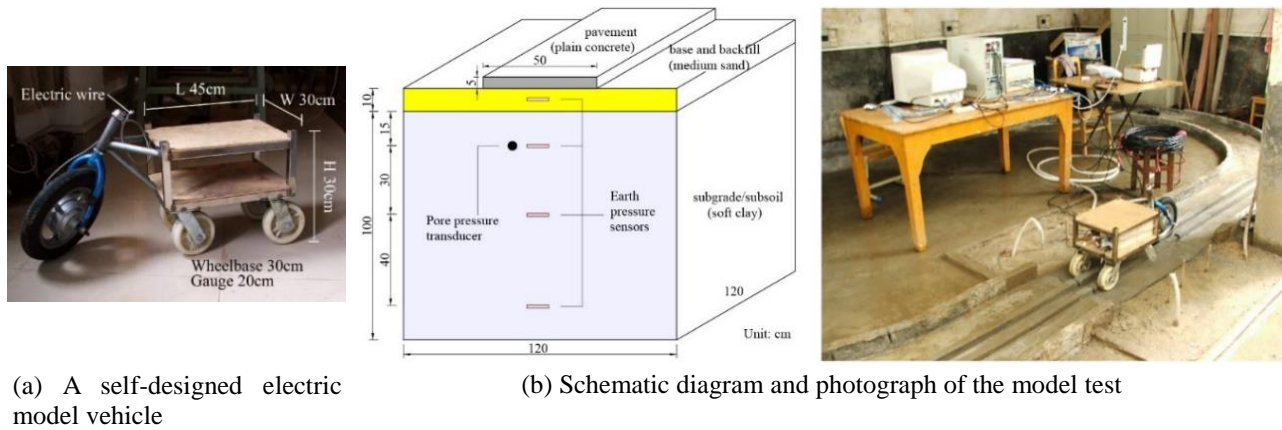


Fig. 5 Schematic diagram of the arrangement of the test setup and photograph of the model test

The small-scale model test was conducted to simulate the stress response within subgrade and subsoil under vehicular loading conditions.

The model scale was 1/8, i.e., the thickness of the structural layers of the road and the size of the model vehicle were 1/8 of the size of the actual objects. Fig. 5(a) shows the custom-designed electric model vehicle used to exert the moving vehicular loads. The model vehicle, with dimensions of  $0.45 \times 0.30 \times 0.30$  m ( $L \times W \times H$ ), was approximately 1/8 of the size of a light truck. The speed of the model vehicle was controlled by the driving current. The weight of the vehicle itself was 15 kg, and the vehicular loads were controlled by adding weights to the vehicle.

Fig. 5(b) illustrates the small-scale model of the pavement and subgrade system. The pit used to set up the soft clay subsoil and medium sand base had dimensions of  $1.2 \times 1.2 \times 1.15$  m ( $L \times W \times H$ ). The boundary was determined according to a static analysis: the vehicular loads were simplified into rectangular uniform loads, and the Boussinesq elastic theory and superposition principle (Arvidsson and Keller 2007, Das 2008) were used to calculate the stress distribution within foundation. The calculated result showed that the additional stresses on the boundaries of the pit were less than 10% of the applied rectangular uniform load; therefore, the boundary effect was assumed to be negligible.

This model test considered the soft clay foundation condition of a highway construction site. The road structures were simplified into three layers: (1) the plain concrete layer simulated the surface layer of the road; (2) the medium sand layer simulated the base and backfill layer beneath the pavement; and (3) the soft clay layer simulated the natural subsoil. The size of each layer is shown in Table 4 and Fig. 5(b). The physical properties of the soft clay and sand used in the model test are shown in Table 2.

The stress data acquisition system consisted of high-precision earth pressure cells and a measurement-controlling unit. The earth pressure cells, which were installed to measure the in-ground total stresses during vehicular loading, were of the piezoelectric type and were 110 mm in diameter and 10 mm thick. The earth pressure cells were sensors filled with de-aired fluid. A pressure transducer measured the pressure change in the fluid when stress was applied to the cell. All of the sensors and

Table 4 Compositions and properties of the material

Layer	Material	Thickness (m)	L × W (m)	Density ( $\text{kg/m}^3$ )	Water content (%)
Pavement	Concrete	0.05	1.2 × 0.5	-	-
Base	Medium sand	0.10	1.2 × 1.2	$1.65 \times 10^3$	8
Foundation	Soft clay	1.00	1.2 × 1.2	$1.60 \times 10^3$	65

transducers were calibrated in the laboratory before use.

### 2.3.2 Model preparation and test procedure

The procedure for the installation of the small-scale test is described below.

(1) The pit was filled with soft clay to form a foundation. The soft clay required watering and was remolded. The clay was filled into the pit in 0.20 m layers. Special care was taken to avoid forming large voids in the foundation.

(2) The measurement sensors and devices were installed. When the soft clay was filled to the predetermined elevation (Fig. 5(b)), the earth pressure sensors were installed. Special care was taken to ensure the horizontal placement of the earth pressure sensors. Once the measurement devices had been installed, the soil was backfilled immediately. The test data were automatically collected by the data acquisition instrument and computer.

(3) The base layer and pavement were set up. After the soft clay foundation had been filled to a thickness of 1.0 m, a 0.10 m sand layer was overlaid on the soft clay to simulate a base layer. The dry density of the sand layer was  $1.60 \times 10^3 \text{ kg/m}^3$  (82.4% degree of compaction). A prefabricated plain concrete slab was paved over the sand layer. A lane of 10.0 m length was set up to guide the model vehicle.

(4) For the static loading of the entire structure, weights were added to the model vehicle to form a static load of 650 N, and then, the load was exerted onto the surface layer. The static loading lasted for 25 days.

### 2.3.3 Test plan

In this small-scale test, the influence of the vehicular load, speed, loading frequency and number of cycles on the dynamic stress response within the soil were investigated.

(1) Weights were added to the model vehicle, and vehicular

Table 5 Test conditions for the small-scale model tests

Group	Test	Vehicular load (N)	Vehicle speed (m/s)	Frequency (Hz)
Group One (M01, 02)	M01	250	2.0	0.2
	M02	650	2.0	0.2
Group Two (M02, 03, 04)	M02	650	2.0	0.2
	M03	650	3.0	0.2
	M04	650	4.0	0.2
Group Three (M05, 02)	M05	650	2.0	0.1
	M02	650	2.0	0.2

loads of 250 and 650 N were obtained. (2) The vehicle speed was set to be 2.0-4.0 m/s. (3) The loading frequencies were set to be 0.1 and 0.2 Hz to simulate the interval times of 10 and 5 s, respectively, between two loading cycles. (4) Three hundred loading cycles were performed in each set of the test. The test conditions for the small-scale model tests are shown in Table 5. Before the next test, the multilayered pavement foundation system and data measurement system were reinstalled.

### 3. Results

#### 3.1 Laboratory cyclic loading model tests

This paper focused on the vertical stress component. There are two types of stresses that need to be defined specifically in this paper: (1) the vertical dynamic additional stress (abbreviated as dynamic stress) response denotes the increase in vertical stress induced by the cyclic load applied on the soil surface; (2) the residual stress denotes the vertical residual additional stress remaining in the soil after the cyclic load has decreased to 0, and the residual stress is a time-dependent variable because it is relieved (decreases) during the soil rebound process. The term elastic after-effect refers to the phenomenon of time-dependent deformations, including the time-dependent increase in deformation during loading and the time-dependent recoverable deformation during unloading (Ling *et al.* 2017, Dong and Huang 2014, Tong and Yin 2013, Wang *et al.* 2008, Yin 2015).

##### 3.1.1 The phenomenon of residual stress accumulation

Figs. 4(d)-4(f) show the additional stress response and deformation of the soil specimen that was subjected to the static load. When the applied load was increased from 50 to 100 kPa (or from 100 to 200 kPa), the stress response increased gradually in the initial stages. However, the stress response subsequently stabilized, although the settlement deformation continued to increase. Significant unrecoverable deformation and residual stress were observed after the applied load was reduced to 0. A slight relief of the residual stress was observed with the time-dependent resilient deformation.

Figs. 4(a)-4(c) present the stress response in the first few cycles of the test C04. The dynamic stress response and soil

deformation showed similar tendencies. During the unloading process, the resilient deformation develops with time, which proves there is elastic aftereffect for the soil material. The residual stress was relieved along with the time-dependent resilient deformation. However, the dynamic stress did not decrease to the initial value of the cycle before the next loading, so the residual stress was superimposed on the subsequent loading cycles. Thus, the two main characteristics of the “dynamic stress accumulation effect” can be summarized as follows: (1) the residual stress increased and accumulated with an increase in the number of loading cycles, and (2) the residual stress was superimposed on the stress response of the subsequent loading cycles, inducing a greater peak stress response.

#### 3.1.2 Residual stress accumulation of soft clay under different loading conditions

Fig. 6 shows the stress response within the soft clay under different loading conditions (tests C01-C06 in Table 3). Fig. 7 shows the deformation during the cyclic loading. These experiments compared the influence of the loading frequency, density, and loading amplitude. Some common characteristics were observed in the results: (1) when the applied loading amplitudes were sufficiently high, the dynamic stresses did not decrease to the initial value of the cycle. Therefore, the residual stresses remained and accumulated in the subsequent cycles; (2) in the initial stages of the cyclic loading, the peak stress responses and residual stresses increased sharply with increases in the number of loading cycles; and (3) later, the peak stresses and residual stresses increased more slowly and tended to become stable.

The soft clay specimens in the cyclic loading stage were still unsaturated (saturation < 95%) even though they had previously been consolidated, which indicated that the dynamic stress accumulation effect was not derived from the occurrence of excess pore water pressure.

(1) The influence of the loading frequency is shown in Figs. 6(a) and 6(b) (as well as in Figs. 6(c) and 6(d)). The deformation behavior of these tests is shown in Fig. 7(a). The resilient deformation and the relief of the residual stress were time-dependent processes. A longer interval between two loadings (a lower loading frequency) results in more resilient deformation after each unloading and thus a greater relief of the residual stress. Moreover, a lower loading frequency also resulted in a slower rate of increase in the residual stress with an increasing number of loading cycles.

(2) The influence of soil density is shown in Figs. 6(c) and e. The deformation behavior of these tests is shown in Fig. 7(b). After the soft clay experienced static compressive loads of 100 and 250 kPa, the dry densities of the soil specimens were  $1.09 \times 10^3$  and  $1.20 \times 10^3$  kg/m<sup>3</sup>, respectively. The residual stress increased more rapidly in the lower-density soil. The higher-density soil exhibited a slightly higher peak stress and a lower residual stress after 2,000 cycles.

(3) The influence of the cyclic loading amplitude is shown in Figs. 6(a), 6(c) and 6(f). The deformation behavior for these tests is shown in Fig. 7(c). A greater cyclic loading amplitude induced a greater accumulation of the residual stress. When the loading amplitude was 5 kPa,

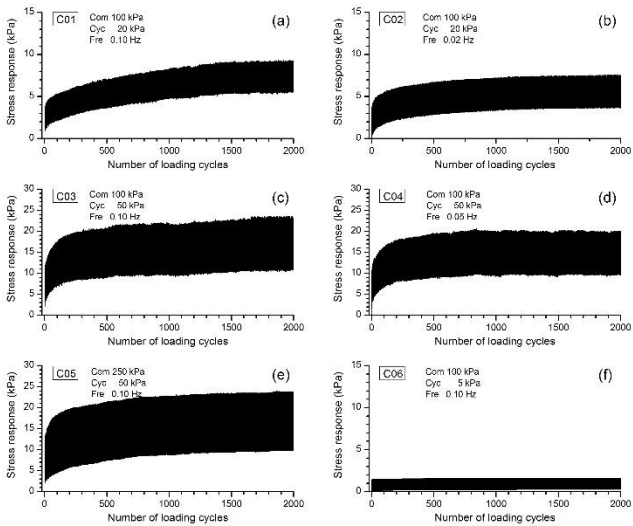


Fig. 6 Dynamic stress response in soft clay specimens under different loading conditions:C01-C06

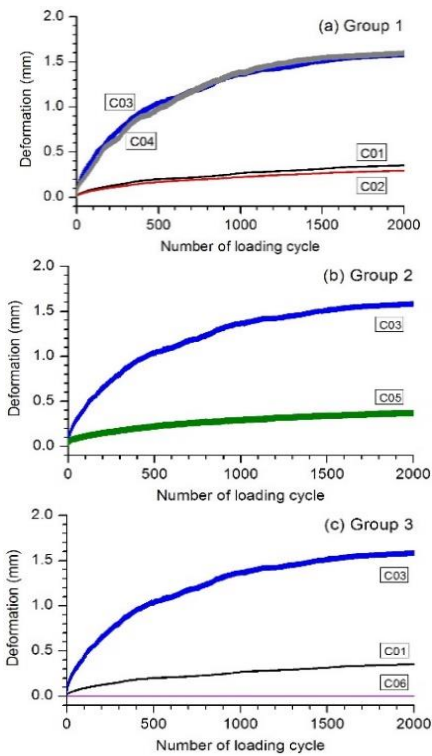


Fig. 7 Deformation behavior of soft clay in tests C01-C06

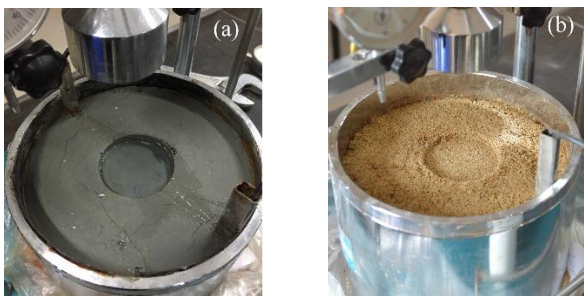


Fig. 8 Failure of the soil specimens when they were subjected to relatively high cyclic loads

the soil exhibited purely elastic behavior after dozens of cycles, and the peak stress and residual stress stabilized. When the loading amplitude was 20 kPa, the peak stress, residual stress and plastic deformation increased rapidly in the first few hundreds of cycles. Then, the peak stress and residual stress stabilized, but the cumulative deformation continued to increase. When the loading amplitude was 50 kPa, the peak stress and residual stress continued to increase until soil failure occurred. The soil failure is shown in Fig. 8(a).

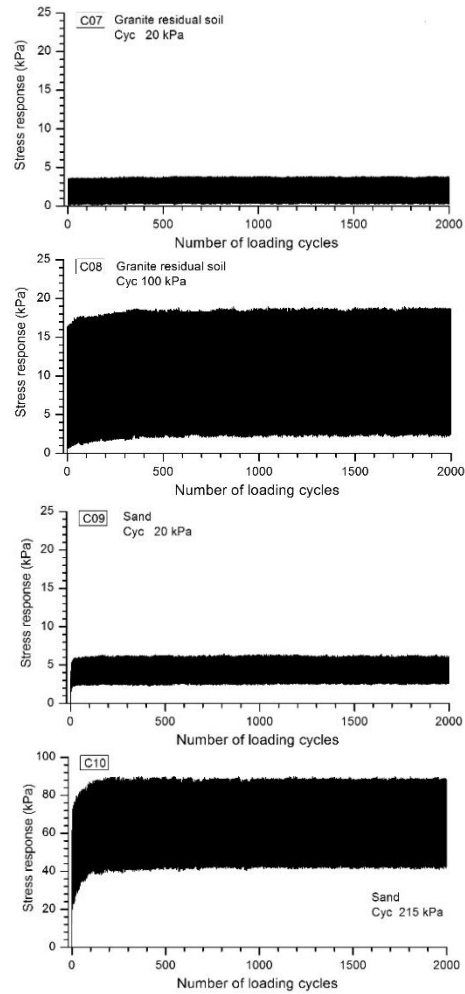


Fig. 9 Dynamic stress response in granite residual soil and medium sand specimens:C07-C10

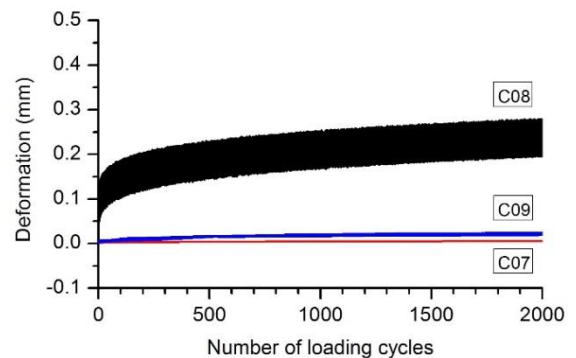


Fig. 10 Deformation behavior of the medium sand and granite residual soil specimens (tests C07-C09)

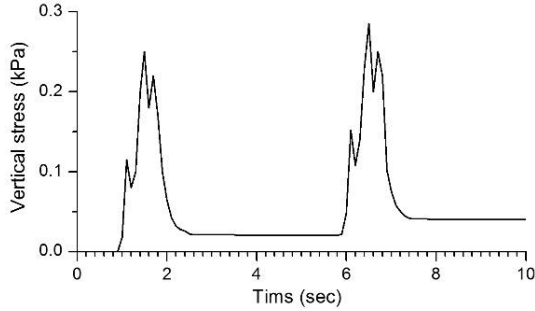


Fig. 11 Real-time response of vertical dynamic stress in clay layer

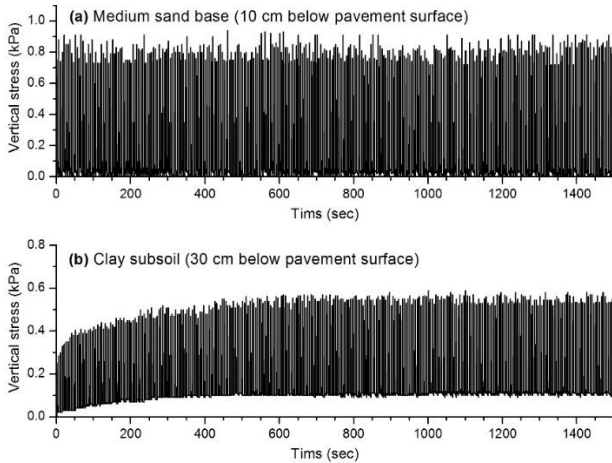


Fig. 12 Vertical stress response within the soft clay subsoil and subgrade sand base (test M02): (a) soft clay subsoil and (b) sand base

3.1.3 Residual stress accumulation of granite residual soil and medium sand

The dynamic stress responses in unsaturated granite residual soil (tests C07-C08) and the unsaturated medium sand (tests C09-C10) are plotted in Fig. 9. The relevant deformation behavior is shown in Fig. 10. The test results indicated that the accumulation of residual stress occurs in not only highly plastic soils with high saturation but also possibly the unsaturated silt and sand. (1) In the case of the granite residual soil, when the cyclic loading amplitude was 20 kPa and there was no accumulation in residual stress or deformation, the accumulation effect occurred when a higher cyclic loading amplitude (50 kPa) was applied. (2) In the case of the medium sand, the dynamic stress accumulation effect occurred when the cyclic loading amplitudes were 20 and 215 kPa. The peak stress responses and residual stresses increased sharply in the first 100 cycles and then stabilized, whereas the plastic deformation continued to increase until soil failure occurred. The failure of the sand soil is shown in Fig. 8(b).

3.2.2 Residual stress accumulation under different loading conditions

Fig. 13 shows the dynamic stress response induced by vehicular loads of 650 N (test M01) and 250 N (test M02). As shown in Fig. 13(a), the dynamic stress accumulation effect occurred 0.15 m below the subsoil surface. The peak stresses and residual stresses increased rapidly in the initial

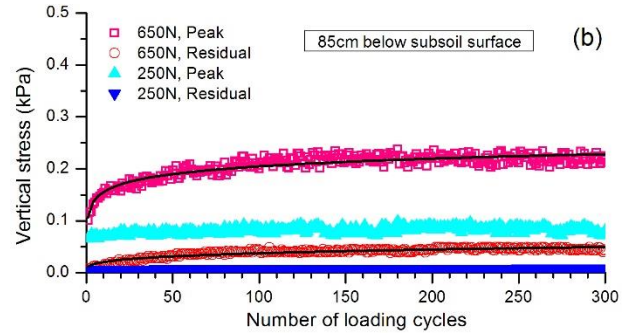
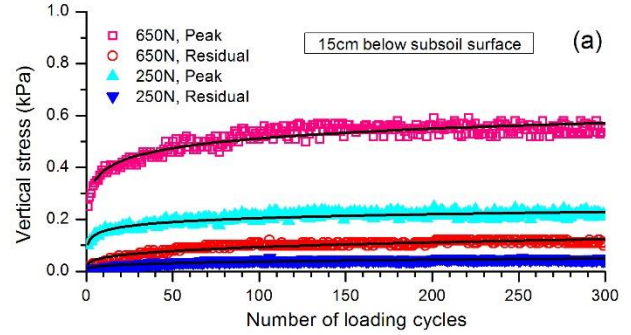


Fig. 13 Vertical stress response under different vehicular loads: (a) 15 cm below the subsoil surface and (b) 85 cm below the subsoil surface

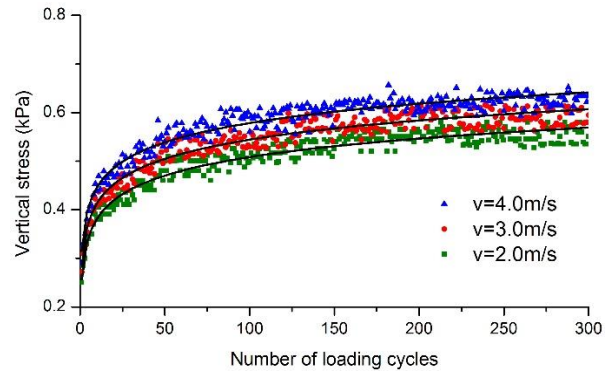


Fig. 14 Influence of running speed on peak stress response (0.15 m below subsoil surface)

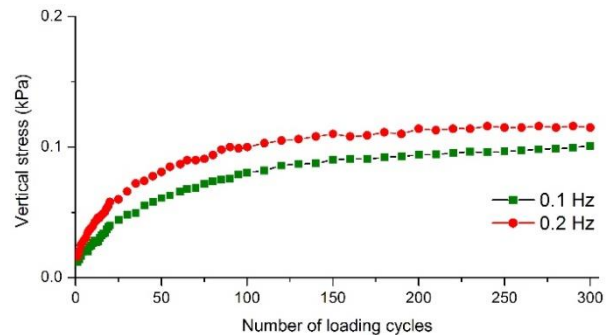


Fig. 15 Influence of loading frequency on the cumulative residual stress

stage of the cyclic loading and then stabilized. When the vehicular load was 250 N, the dynamic stress accumulation effect was less significant, and the cyclic stress response reached a stable state more rapidly. Fig. 13(b) shows that at

a deeper position of 0.85 m below the subsoil surface, the dynamic stress accumulation effect occurred when the vehicular load was 650 N, whereas the dynamic stress accumulation effect did not occur when the vehicular load was 250 N.

The influence of vehicle speed on the peak stress is shown in Fig. 14. The peak stress increased with an increase in vehicle speed. Due to the uneven surface of the concrete pavement, the moving vehicle might induce additional impact loads, which would cause greater stress responses than under the static loading condition (Lu *et al.* 2012, Zhu *et al.* 2011).

Fig. 15 shows the influence of the loading frequency on the development of residual stresses. The testing position was 0.15 m below the subsoil surface, and the vehicular load was 650 N. A higher loading frequency (shorter interval time) led to a faster accumulation rate for the residual stress.

## 4. Discussion

### 4.1 Dynamic stress accumulation effect

The dynamic stress accumulation effect includes two main characteristics: (1) the residual stress accumulates and increases with an increasing number of loading cycles, and (2) the residual stress is superimposed on the stress response of the subsequent loading cycles, inducing a greater peak stress response.

The occurrence and accumulation of the residual stress within soils can be explained as follows. When the soil shows plastic deformation under cyclic loading, the soil particles rotate and rearrange, thereby inducing structural stresses within the material (Michalowski and Nadukuru 2012, Le *et al.* 2015, Tang *et al.* 2015). The soil exhibits time-dependent resilient deformation during the interval between two loadings, and the energy stored in the deformed mineral particles is relieved. A part of the internal stress is relieved with the time-dependent resilient deformation. The remaining residual stress is superimposed on the next loading cycle. When the next loading occurs, greater movement of the soil particles causes increased residual stress. Therefore, residual stress accumulation is observed from the macro perspective.

A comparison was made between test C01 (Fig. 6(a)) and test C07 (Fig. 9(a)). Under the same cyclic load of 20 kPa, the soft clay exhibited cumulative deformation and a dynamic stress accumulation effect, whereas the granite residual soil exhibited purely elastic behavior without a dynamic stress accumulation effect. This comparison indicates that the dynamic stress accumulation effect is less significant in the soils with higher integral rigidity and stiffness. Moreover, the dynamic stress accumulation effect will not occur if the resilient deformation recovers before the next loading.

In the small-scale model test, the stiffness of the medium sand was greater than the stiffness of the soft clay. Because the cyclic loads were relatively low (250–650 N, which induced dynamic stresses of less than 1 kPa in the sand base layer), there was no dynamic stress accumulation

effect within the sand base, indicating again that the performance of the dynamic stress accumulation effect is closely related to the stiffness of the soil. The dynamic stress in the subsoil decreases to the initial level of the cycles in the later stages of the cyclic loading, reflecting that the compaction of the soil material under cyclic loading contributed to the stabilization of the dynamic additional stress response.

The dynamic stress accumulation effect is one of the characteristics of “under-compacted soil”. Under-compaction is a relative concept that is determined based on a comparison between the load and the elastic limit of the material. If the soil shows unrecoverable deformation after unloading, the soil is defined as under-compacted.

In summary, two conditions must be met for the dynamic stress accumulation response to occur within the soil material: (1) the soil shows plastic deformation under cyclic loading; and (2) the residual stress in the material cannot be completely relieved before the next loading. In subsequent subsections, the factors that influence the performance of dynamic stress accumulation were analyzed, including the load, vehicle speed, loading frequency and number of loading cycles.

### 4.2 Influence of the load

The experimental results of test C07 in the laboratory model tests (Fig. 9(a)) showed that if the cyclic load was relatively low (20 kPa), neither the cumulative deformation nor the dynamic stress accumulation effect occurred. The dynamic stress accumulation effect occurred when the load was higher.

The experimental results of tests M01 and M02 in the small-scale model test (Fig. 13) demonstrate the difference between the dynamic stress responses induced by vehicular loads of 650 N and 250 N. The dynamic stress accumulation effect occurred 0.15 m below the subsoil surface (Fig. 13(a)). The lower vehicular load induced a lower stress response, and the peak stress and residual stress reached a stable state more rapidly. The accumulation of residual stresses within the shallow foundation varies because of the magnitude of the loads. However, at the deeper position of 0.85 m below the subsoil surface, only the vehicular load of 650 N resulted in the accumulation of residual stresses.

The influence of load indicates that the dynamic stress accumulation effect occurs only if the cyclic load exceeds a threshold stress value. Considering that the residual stress occurs in conjunction with plastic deformation, this threshold stress value might be in conformity with the “cyclic threshold stress” in shakedown theory (Shahu *et al.* 2000, Tang *et al.* 2015, Werkmeister *et al.* 2005), i.e., the greatest stress that can be applied to a material without causing permanent deformation. The stress response within the medium sand base in the small-scale model test confirmed this deduction. The threshold load required to incur the dynamic stress accumulation effect in the sand would be greater than the threshold load required to incur the dynamic stress accumulation effect in the soft clay because the stiffness of the sand was considerably higher. Thus, under the same vehicular load of 650 N, the dynamic

stress accumulation effect occurred in soft clay subsoil but did not occur in the sand base (Fig. 12). However, tests C09 and C10 in the laboratory model test (Figs. 9c and d) showed that the dynamic stress accumulation effect would be also observed in the sand if the cyclic loads were high. Similar test results were obtained by Shoop *et al.* (2009) and Thakur *et al.* (2012) who observed the dynamic stress accumulation effect in cohesionless soil if the loads were relatively high.

This subsection revealed that there is a threshold state in which the dynamic stress accumulation effect occurs within subgrade soil only if the external load exceeds the cyclic threshold stress. A higher cyclic loading amplitude causes greater accumulation of residual stress.

#### 4.3 Influence of frequency

Resilient deformation and residual stress relief are time-dependent processes. The accumulation of the residual stress is influenced by the loading frequency (external cause) and the time needed for complete stress relief (internal cause).

Situation one: The soil exhibits elastic behavior under a relative low stress level (i.e., the soil deformation would recover completely in a finite time period).

(1) If the elastic deformation showed complete recovery (and the residual stress was completely relieved) during the interval between two loadings, there would be no dynamic stress accumulation effect in the subgrade soil.

(2) If the elastic deformation did not completely recover (and the residual stress was not completely relieved) before the next loading, the residual stress would be superimposed onto the next cycle. A higher loading frequency means a shorter time for stress relief, thus inducing a greater accumulation rate of the residual stress with an increasing number of loading cycles. However, under these conditions, the residual stress might be sufficiently small to be neglected, and the residual stress might be completely relieved in a finite time period as the repeated loading stops.

Situation two: The soil shows unrecoverable deformation when subjected to a relatively high load. In this situation, there would be permanent residual stresses within the material. The residual stress would be superimposed onto the subsequent cycles. A higher loading frequency induces a greater accumulation rate and a greater amount of residual stress during cyclic loading.

#### 4.4 Influence of soil deformation and number of loading cycles

In the initial stage of cyclic loading, the dynamic peak stresses and residual stresses increase quickly, after which the rate of increase gradually decreases. The stress responses tend to be stable after the long-term loading. The deformation and stress response in the soil due to the vehicular load are dynamic processes (Karmakar and Kushwaha 2007), and thus, the internal effect should be considered.

When the soil experiences a particular set of variable loads, the soil particles may rotate and rearrange. Because this plastic strain is incompatible with the elastic strain

during unloading, a residual stress field remains in the structure upon unloading (Michalowski and Nadukuru 2012, Tang *et al.* 2015). In the initial stage of cyclic loading, increments in the plastic deformation and residual stress were observed in each cycle, and the residual stresses were superimposed onto the subsequent cycles. However, when applying low-to-medium cyclic loads, the soil deformation stabilized and reached the shakedown state (Tang *et al.* 2015, Werkmeister *et al.* 2005) in certain cases after long-term cyclic loading. Thus, the stress response (residual stress and peak stress) was stable due to the increase in soil stiffness.

In addition, the peak stresses also increased during the cyclic loading (Figs. 6, 10, 13 and 14). The residual stress was superimposed on the stress response of the subsequent loading cycles, thus inducing a greater peak stress response. In addition to the contribution from the increasing residual stress, the increased peak stress might be due to the higher soil stiffness and greater stress transmission in the structure (Naveed *et al.* 2016), as shown in Figs. 4(d) and 4(e). In an under-compacted soil material, the resisting and dissipative mechanism (i.e., frictional displacement and viscous flow of the soil particles) causes the loading energy to dissipate (Lu and Chung 2014, Pisanò and Jeremić 2014, Tang *et al.* 2015) and reduces the stress transmission in the material. Soil compaction occurs during the cyclic loading, and a higher degree of compaction is expected to increase the stiffness and reduce the plastic deformation (Chen and Chung 2012, Lu and Chung 2014). Thus, the dissipative energy in each loading decreases as the cyclic loading continues. In this sense, the increase in the peak stress response might also be attributed to the increase in the soil stiffness and the reduction in the dissipative energy, thereby inducing a greater stress transmission within the soil material.

The stress response under static loading conditions (Figs. 4(d)-4(f)) shows that the increase in the stress response within the soil was concurrent with the increase in the deformation (densification) of the soil. However, the stress response subsequently stabilized even though the soil deformation continued to increase. This phenomenon indicates that the soil deformation is an essential but not sufficient condition of the increase in stress response.

#### 4.5 Related engineering suggestions

The vertical stress component is typically the maximum stress in subgrade and subsoil (Alakukku *et al.* 2003, Chai and Miura 2002, Shoop *et al.* 2009), and this stress component is considered the major source of subgrade and subsoil settlement. The magnitude of the vertical residual stress should be considered because the superposition of the residual stresses and the overburden stresses might induce unexpected foundation settlement (Li and Liu 2014).

According to the experimental results and analysis, the dynamic stress accumulation effect is more significant within the soils that are prone to deform under loading. Some suggestions for reducing the negative influence of the dynamic stress accumulation effect on the stability of subgrade and subsoil are as follows: (1) For the soft subsoil layer, reinforcing methods (such as the dynamic compaction

method, drainage consolidation method, and complex foundation method (Li *et al.* 2015, Lu and Chung 2014, Zou *et al.*, 2005) can be applied to enhance the stiffness and bearing capacity of the foundation. (2) For the subgrade layer, a static compaction method and vibratory compaction method (Eguchi and Muro 2007, Zou *et al.* 2005) can be applied to obtain a high degree of compaction of the soil with the optimum moisture content. In addition, reinforcement methods, such as the cemented soil method and geocell-reinforced method (Chai and Miura 2002, Hendry *et al.* 2013, Mittal and Meyase 2012, Tafreshi and Norouzi 2015, Thakur *et al.* 2012), can be applied to increase the integral rigidity of the materials. If the subgrade soil has been compacted to a relatively high degree during the construction period, the dynamic stress accumulation effect during the traffic period might be not significant. (3) For the pavement and base layer, the pavement and base course are the layers directly subjected to the vehicular load and should thus be designed as layers that can sharply dissipate the dynamic additional stresses near the loading area.

## 5. Conclusions

The dynamic stress accumulation effect might occur within the subgrade and subsoil when the ground is subjected to repeated vehicular loads. The dynamic stress accumulation effect illustrates that: (1) the residual stress accumulates and increases with an increasing number of loading cycles, and (2) the residual stress is superimposed on the stress response of the subsequent loading cycles, inducing a greater peak stress response.

Two conditions cause the occurrence of the dynamic stress accumulation effect: (1) the soil exhibits plastic deformation under cyclic loading; and (2) the residual stress in the material cannot be completely relieved before the next loading.

Factors influencing the performance of dynamic stress accumulation include the soil type, magnitude of the load, vehicle speed, loading frequency and number of loading cycles. A threshold state exists regarding the stress accumulation effect. The stress accumulation effect only occurs if the external load exceeds the cyclic threshold stress. Higher loading frequencies result in a more rapid rate of residual stress accumulation. In addition, the dynamic stress accumulation effect is more significant within the soils that are prone to deform under loading.

In addition to the superposition of the increasing residual stress, the increasing peak stress might account for the increasing stiffness of the soil material. A higher compactness and stiffness contribute to greater stress transmission in the structure. The increase in stiffness and reduction in the dissipative energy induce a greater stress transmission within the soil material.

## Acknowledgements

This study was supported by the National Natural Science Foundation of China (Grant no. 41572277), the

Natural Science Foundation of Guangdong Province, China (Grant no. 2015A030313118), the Specialized Research Fund for the Doctoral Program of Higher Education of China (Grant no. 201201711110031) and the Science and Technology Program of Guangzhou, China (Grant no. 201607010023).

## References

- Abdelkrim, M., Bonnet, G. and de Buhan, P. (2003), "A computational procedure for predicting the long term residual settlement of a platform induced by repeated traffic loading", *Comput. Geotech.*, **30**(6), 463-476.
- Alakukku, L., Weisskopf, P., Chamen, W.C.T., Tijink, F.G.J., van der Linden, J.P., Pires, S., Sommer, C. and Spoor, G. (2003), "Prevention strategies for field traffic-induced subsoil compaction: A review", *Soil Till. Res.*, **73**(1-2), 145-160.
- Arvidsson, J. and Keller, T. (2007), "Soil stress as affected by wheel load and tyre inflation pressure", *Soil Till. Res.*, **96**(1-2), 284-291.
- Chai, J.C. and Miura, N. (2002), "Traffic-load-induced permanent deformation of road on soft subsoil", *J. Geotech. Geoenviron. Eng.*, **128**(11), 907-916.
- Chen, P.H. and Chung, D.D.L. (2012), "Dynamic mechanical behavior of flexible graphite made from exfoliated graphite", *Carbon*, **50**(1), 283-289.
- Cui, X.Z., Zhang, N., Zhang, J. and Gao, Z.J. (2014), "In situ tests simulating traffic-load-induced settlement of alluvial silt subsoil", *Soil Dyn. Earthq. Eng.*, **58**(1), 10-20.
- Das, B.M. (2008), *Advanced Soil Mechanics*, Taylor and Francis.
- Dong, Q. and Huang, B. (2014), "Laboratory evaluation on resilient modulus and rate dependencies of RAP used as unbound base material", *J. Mater. Civil Eng.*, **26**(2), 379-383.
- Eguchi, T. and Muro, T. (2007), "Measurement of compacted soil density in a compaction of thick finishing layer", *J. Terramech.*, **44**(5), 347-353.
- Garg, N., Pecht, F. and Jia, Q. (2010), "Subgrade stress measurements under heavy aircraft gear loading at FAA national airport pavement test facility", *Proceedings of the GeoShanghai 2010: Paving Materials and Pavement Analysis*, Shanghai, China, May.
- Guo, L., Wang, J., Cai, Y.Q., Liu, H.L., Gao, Y.F. and Sun, H.L. (2013), "Undrained deformation behavior of saturated soft clay under long-term cyclic loading", *Soil Dyn. Earthq. Eng.*, **50**(1), 28-37.
- Hendry, M.T., Martin, C.D. and Barbour, S.L. (2013), "Measurement of cyclic response of railway embankments and underlying soft peat foundations to heavy axle loads", *Can. Geotech. J.*, **50**(5), 467-480.
- Hu, Y.Y. (2010), "Long-term settlement of soft subsoil clay under rectangular or semi-sinusoidal repeated loading of low amplitude", *Can. Geotech. J.*, **47**(11), 1259-1270.
- Karmakar, S. and Kushwaha, R.L. (2007), "Development and laboratory evaluation of a rheometer for soil visco-plastic parameters", *J. Terramech.*, **44**(2), 197-204.
- Le, T.M., Fatahi, B., Disfani, M. and Khabbaz, H. (2015), "Analyzing consolidation data to obtain elastic viscoplastic parameters of clay", *Geomech. Eng.*, **8**(4), 559-594.
- Li, Z.M. and Liu, J.X. (2014), "Experimental study of pore water pressure variation law of muck under high energy impact", *Rock Soil Mech.*, **35**(2), 339-345.
- Ling, X., Li, P., Zhang, F., Zhao, Y., Li, Y. and An, L. (2017), "Permanent deformation characteristics of coarse grained subgrade soils under train-induced repeated load", *Adv. Mater. Sci. Eng.*, (7), 1-15.

- Liu, J.K. and Xiao, J.H. (2010), "Experimental study on the stability of railroad silt subgrade with increasing train", *J. Geotech. Geoenviron. Eng.*, **136**(6), 833-841.
- Lu, S. and Chung, D.D.L. (2014), "Viscoelastic behavior of silica particle compacts under dynamic compression", *J. Mater. Civ. Eng.*, **26**(3), 551-553.
- Lu, Z., Yao, H.L., Wu, W.P. and Cheng, P. (2012), "Dynamic stress and deformation of a layered road structure under vehicle traffic loads: Experimental measurements and numerical calculations", *Soil Dyn. Earthq. Eng.*, **39**(1), 100-112.
- Michalowski, R.L. and Nadukuru, S.S. (2012), "Static fatigue, time effects, and delayed increase in penetration resistance after dynamic compaction of sands", *J. Geotech. Geoenviron. Eng.*, **138**(5), 564-574.
- Ministry of Transport of the People's Republic of China (2012), *China Verification Regulation of Lever Pressure Instrument (JJG107-2012)*, China Communications Press, Beijing, China.
- Ministry of Water Resources of the People's Republic of China (1999), *China Standard for Soil Test Method (GBT 50123-1999)*, China Planning Press, Beijing, China.
- Mittal, S. and Meyase, K. (2012) "Study for improvement of grounds subjected to cyclic loads", *Geomech. Eng.*, **4**(3) 191-208.
- Naveed, M., Schjønning, P., Keller, T., de Jonge, L.W., Moldrup, P. and Lamandé, M. (2016), "Quantifying vertical stress transmission and compaction-induced soil structure using sensor mat and X-ray computed tomography", *Soil Till. Res.*, **158**(1), 110-122.
- Pisanò, F. and Jeremić, B. (2014), "Simulating stiffness degradation and damping in soils via a simple visco-elastic-plastic model", *Soil Dyn. Earthq. Eng.*, **63**, 98-109.
- Puppala, A.J., Saride, S. and Chomtid, S. (2009), "Experimental and modeling studies of permanent strains of subgrade soils", *J. Geotech. Geoenviron. Eng.*, **135**(10), 1379-1389.
- Sas W., Głuchowski A., Bursa, B. and Szymański A. (2017), "Energy-based analysis of permanent strain behaviour of cohesive soil under cyclic loading", *Acta Geophys.*, **65**(2), 331-344.
- Shahu, J.T. and Kameswararao, N.S.V. (2000), "A rational method for design of railroad track foundation", *Soil. Found.*, **40**(6), 1-10.
- Shoop, S., Coutermarsh, B., Diemand, D. and Way, T. (2009) "Using soil stress state transducers in freezing ground", *Proceedings of the Cold Regions Engineering 2009: Cold Regions Impacts on Research, Design, and Construction*, Duluth, Minnesota, U.S.A., August-September.
- Suiker, A.S.J., Selig, E.T. and Frenkel, R. (2005), "Static and cyclic triaxial testing of ballast and subballast", *J. Geotech. Geoenviron. Eng.*, **131**(6), 771-782.
- Sun, X.H., Han, J., Kwon, J., Parsons, R.L. and Wayne, M.H. (2015), "Radial stresses and resilient deformations of geogrid-stabilized unpaved roads under cyclic plate loading tests", *Geotext. Geomembr.*, **43**(5), 440-449.
- Tafreshi, S.N.M. and Norouzi, A.H. (2015), "Application of waste rubber to reduce the settlement of road embankment", *Geomech. Eng.*, **9**(2), 219-241.
- Tang, L.S., Chen, H.K., Sang, H.T., Zhang, S.Y. and Zhang, J.Y. (2015), "Determination of traffic-load-influenced depths in clayey subsoil based on the shakedown concept", *Soil Dyn. Earthq. Eng.*, **77**(1), 182-191.
- Tang, L.S., Xu, T., Lin, P.Y. and Yu, H.T. (2009), "Studies on dynamic stress characters of layered road system under traffic loading", *Chin. J. Rock Mech. Eng.*, **28**(S2), 3876-3884 (in Chinese).
- Tang, Y.Q., Cui, Z.D., Zhang, X. and Zhao, S.K. (2008), "Dynamic response and pore pressure model of the saturated soft clay around the tunnel under vibration loading of Shanghai subway", *Eng. Geol.*, **98**(3-4), 126-132.
- Thakur, J.K., Han, J., Pokharel, S.K. and Parsons, R.L. (2012), "Performance of geocell-reinforced recycled asphalt pavement (RAP) bases over weak subgrade under cyclic plate loading", *Geotext. Geomembr.*, **35**(1), 14-24.
- Tong, F. and Yin, J.H. (2013), "Experimental and constitutive modeling of relaxation behaviors of three clayey soils", *J. Geotech. Geoenviron. Eng.*, **139**(11), 1973-1981.
- Wang, N., Zhang, W., Gu, X. and Zeng, Y. (2008), "Model test on inundation swelling deformation of expansive soil foundation", *J. Highway Transp. Res. Dev.*, **3**(2), 72-76.
- Werkmeister, S., Dawson, A.R. and Wellner, F. (2005), "Permanent deformation behaviour of granular materials", *Road Mater. Pavement Des.*, **6**(1), 31-51.
- Wiermann, C., Way, T.R., Horn, R., Bailey, A.C. and Burt, E.C. (1999), "Effect of various dynamic loads on stress and strain behavior of a Norfolk sandy loam", *Soil Till. Res.*, **50**(2), 127-135.
- Yin, J.H. (2015), "Fundamental issues of elastic viscoplastic modeling of the time-dependent stress-strain behavior of geomaterials", *J. Geomech.*, **15**(5), A4015002.
- Zhang, Q.H., Tang, L.S., Wu, Y.G. and Yin, J.Z. (2009), "Research on accumulation effect of dynamic stress in plastic soil under repeated dynamic loads and its quantitative model", *Hydrogeol. Eng. Geol.*, **36**(6), 76-79.
- Zhu, Z.Y., Ling, X.Z., Chen, S.J., Zhang, F., Wang, Z.Y., Wang, L.N. and Zou, Z.Y. (2011), "Analysis of dynamic compressive stress induced by passing trains in permafrost subgrade along Qinghai-Tibet Railway", *Cold Reg. Sci. Technol.*, **65**(3), 465-473.
- Zou, W.L., Wang, Z. and Yao, Z.F. (2005), "Effect of dynamic compaction on placement of high-road embankment", *J. Perform. Construct. Fac.*, **19**(4), 316-323.

CC